Springer

Journal of
Mechanical
Science and
Technology

Journal of Mechanical Science and Technology 23 (2009) 1102~1111

www.springerlink.com/content/1738-494x
DOI 10.1007/s12206-008-1121-2

Novel scan path generation method based on area division for SFFS †

Kyung-Hyun Choi[1], Hyung-Chan Kim[2,*], Yang-Hoi Doh[2] and Dong-Soo Kim[3]

[1]*Department of Mechanical Engineering, Cheju National University, 66 Jejudaehakno, Jeju-si, Jeju-do, Korea*
[2]*Department of Electronic Engineering, Cheju National University, 66 Jejudaehakno, Jeju-si, Jeju-do, Korea*
[3]*Nano-Mechanical System Research Division, Korea Institute of Machinery & Materials, 104, Sinseongno, Yuseong-Gu, Deajeon, 305-343, Korea*

(Manuscript Received March 27, 2007; Revised November 21, 2008; Accepted November 26, 2008)

Abstract

A solid freeform fabrication (SFF) system using selective laser sintering (SLS) is currently recognized as a leading process of fabrication using variable materials, and SLS extends the application to machinery and automobiles. Due to the time delay in the sintering process, shrinkage and warping often occur. Curling also occurs due to laser and scan delays. These problems affect not only the accuracy of the fabricated product but also the total system efficiency. These deficiencies can be overcome by reducing the total processing time of the SFF system. To accomplish this, the laser scanning time, from mark (laser on) to jump (laser off), must be reduced as it contributes the major part of the total processing time. This can be done by employing area division scan path generation, which promotes digital efficiency. A simulation and an experiment was carried out in this study to evaluate the developed scan path method.

Keywords: Solid freeform fabrication system; Area division scan path; Digital mirror system

1. Introduction

Selective laser sintering (SLS) is a leading process in the new field of solid freeform fabrication (SFF). SLS is an additive process that produces parts directly from the CAD model by melting or by sintering layers of a powder together with the use of a laser beam [1]. The laser scanner, which considerably affects the precision and efficiency of the SLS machine, is used in both the generation of scan paths from a sliced section and in the scan control to ensure that the generated paths are followed. To generate these scan paths, the scan spacing, the diameter of the laser beam, and the scan speed have to be considered. With these parameters scan paths are generated, in order to ensure that these scan paths are being followed a scan control is needed, which ensures the fabricated surface to absorb fine energy and enhancement in dimensional accuracy. The scan path generation algorithm that is used affects the accuracy and total time of manufacturing.

The use of the SLS machine, which uses sintering powder and thermal energy, entails a time delay in the sintering process. This results in shrinkage, curling, and warping owing to thermal distribution. The reduction of thermal distribution can enhance the precision and quality of the fabricated part. To do this, it is important to quickly scan the surface of the powder. The shorter the fabricating time in one layer, the lesser the thermal distribution will be, resulting in better quality. To generate scan paths fast, adaptive paths according to the geometrical shape of each layer are needed [1-3]. Intelligent scan path method can reduce the curling, shrinkage, and growth of the fabricated part [4]. These dimensional errors were eliminated by optimizing the laser power, scan spacing, and scan speed of the different regions, even in the same layer. The Bonus-Z model was also developed to compensate for bottom

† This paper was recommended for publication in revised form by Associate Editor Dae-Eun Kim

*Corresponding author. Tel.: +82 64 754 3713, Fax.: +82 64 756 3886
E-mail address: khchoi@cheju.ac.kr

growth at several bottom surfaces. The quality of the fabricated part can be enhanced by generating a scan path from the directly sliced section of the STL file [5]. This was done to compensate for the deterioration of the quality of the final part when the scan path was generated from the sliced section of the STL file. Park's work remarkably improved the quality of the fabricated part using complex geometry. Curling and shrinkage phenomena can be further reduced by minimizing the differences between the thermal stresses in the neighboring regions of the same layer [6]. To do this, a fractal scan path was generated instead of a linear scan path to reduce the differences in thermal distribution. An effective scan method can be derived by generating a scan path with offsets from the contour, such that the inner and outer surfaces of the contour are scanned by using an offset value. This method proved to be faster, and the resulting scanned surfaces were finer than those produced by linear scan paths [6].

A scan path is formed through the mark and the jump, which move from one scanning spot to the next scanning spot. The processing time can be shortened by removing the jump section of the unnecessary laser through the existing scan path creation method. Such jump section can also be made smaller through the formation of an area division scan path, by rearranging the areas that minimize the jump section. Separating the scan section by area and rearranging the scan path make it possible to come up with the area division scan path for the digital mirror system, to remove the unnecessary jump section, and to minimize the transfer section. They also serve as proof of the shortening of the total processing time, and of the processing accuracy and efficiency [1-3].

This study describes the creation of the area division scan path, which is needed to rearrange the existing scan path. The suggested method can shorten the total processing time and increase the processing accuracy, as well as the scan efficiency. To evaluate the method, models were fabricated by applying different scan methods. These fabricated models were then inspected and used for simulation and experimentation. The results of the simulation and experiment were later compared.

2. Previous study

2.1 Laser scan system

A typical laser scan system for SFFS is shown in Fig. 1. This system consists of a CO_2 laser, an optic for beam transfer, and a scanner that takes charge of beam spot position control on a two-dimensional plane. The fabrication process is completed by applying the following procedure on all the layers: after one layer is sintered through laser scanning, fresh powder is spread on the following layer with the use of a roller, and the layer is scanned [1].

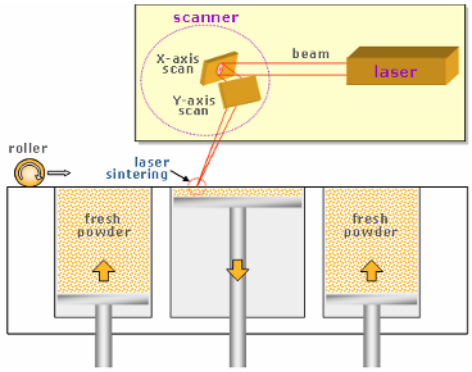

Fig. 1. Schematic diagram of SFFS

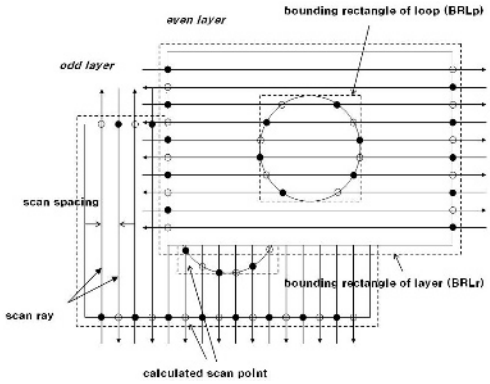

Fig. 2. Calculated scan points and terminologies.

2.2 Scan path generation

After the STL file is converted from the three-dimensional modeling part by using a commercial CAD software, a scan path is generated by calculating the scan points in each layer that has been sliced according to its stacking thickness [1-3].

The scan path generation algorithm for a sliced section is that produced when a scan ray moving through every scan space intersects a contour segment, and when scan points are calculated continually, as shown in Fig. 2. To reduce the calculation time of the intersection between a scan ray and a contour segment, BRLp (bounding rectangle of loop) was defined as the

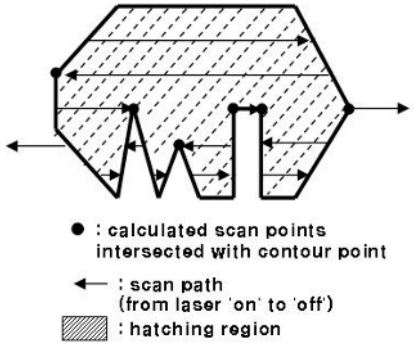

Fig. 3. Wrong scan paths.

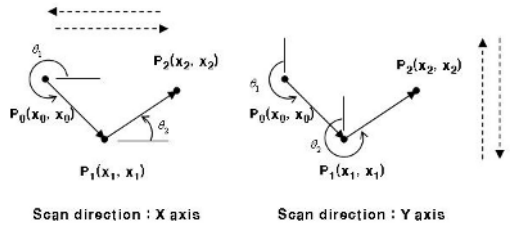

Fig. 4. Vector representation between neighboring scan points.

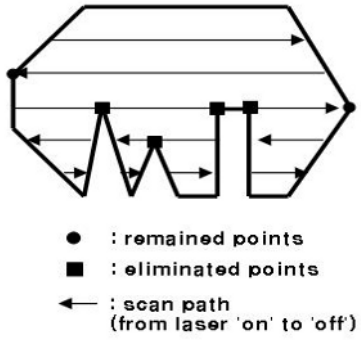

Fig. 5. Modified scan paths.

$$\theta_1 = \cos^{-1}\left(\frac{x_1 - x_0}{\sqrt{(x_1 - x_0)^2 + (y_1 - y_0)^2}}\right) \quad (1)$$

$$\theta_1 = \cos^{-1}\left(\frac{x_2 - x_1}{\sqrt{(x_2 - x_1)^2 + (y_2 - y_1)^2}}\right) \quad (2)$$

$$0^\circ < \theta_1 \le 180^\circ \text{ and } 0^\circ \le \theta_2 < 180^\circ \quad (3)$$

$$180^\circ < \theta_1 \le 360^\circ \text{ and } 180^\circ \le \theta_2 < 360^\circ \quad (4)$$

rectangular boundary of each loop, which consists of four segments. If the scan ray does not intersect any of the four segments of BRLp, the calculation process will skip this loop and will proceed to the next loop or layer. First, in each sliced section, all the intersection points between the scan rays that are parallel with the X-axis and the contour points are calculated. The scan path in each layer is calculated by sorting the obtained points in ascending and descending order from the starting point to the end point of the BRLr (bounding rectangle of layer) boundary. At this point, the number of calculated points has to be even (laser "on" and "off"). After sorting and saving the obtained scan points, the scanner will operate from one point to the next point, with the laser continuously being turned "on" and "off."

However, in the method used to find the intersection points between simple scan rays and contour segments, if the contour points are adopted as scan points, as shown in Fig. 3, severe errors will occur. This problem does not occur when the scan points being calculated are not between contour points but between a contour segment and a scan ray. It occurs, however, when the scan points being calculated are between contour points and scan rays. This results in a wrong scan sequence of the "jump" and "mark" commands, as shown in Fig. 3. To address this problem, when contour points are adopted as scan points, if the condition reflected in Eq. (3) is satisfied, it has to be adopted; otherwise, it has to be disposed of. Fig. 4 shows the vector representation among the three points. Eq. (1) and Eq. (2) represent each angle between each vector and the X-axis and Y-axis, respectively. The scan path of each even layer is along the X-axis, and along the Y-axis for each odd layer, as shown in Fig. 2. Therefore, θ_1 and θ_2 are differently defined, as shown in Fig. 4. Fig. 5 shows the modified scan path from the wrong path in Fig. 3 using Eq. (1), Eq. (2), and Eq. (3) [7-10].

3. Scan path generation algorithm development based on area division

3.1 The area division scan path efficiency

When the two-dimensional slicing cross-section information creates scan paths of equal areas, the laser scan time is decided based on the laser mark, for processing purposes. The laser jump for transfer and the delay time follow this scan path. That is, the total processing efficiency is enhanced because a distortion that reduces the unnecessary laser jump occurs through the delay, also decreasing the time required for the whole process.

A scan path with a simple-zigzag pattern, such as that in Fig. 6, involves much transferring of unnecessary scan paths. It therefore produces many unnecessary jumps. In this study, an algorithm that occurs in the minimum laser transfer section was developed by rearranging the scan paths with a zigzag mode, which can serve as proof of the efficiency of the scan method [11].

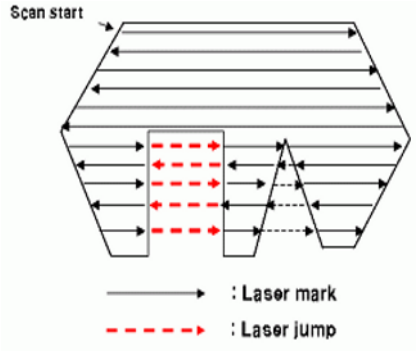

Fig. 6. Simple scan path.

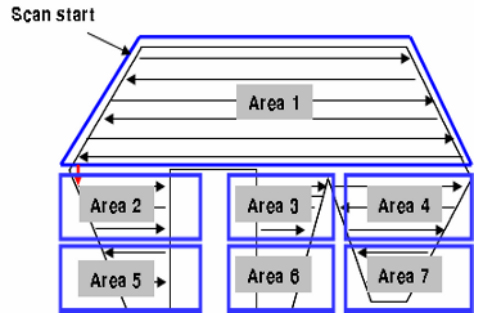

Fig. 7. Reconstructed scan path.

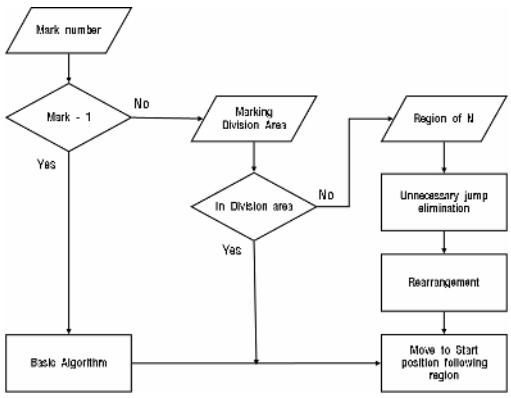

Fig. 8. The area division flow chart.

3.2 The Area division scan path algorithm

Fig. 7 shows a method that can be used to complete the area division so as to remove the unnecessary jump area. The scan paths in each scan area were rearranged based on the areas, which were classified into Area 1, Area 2, Area 3, and Area 4. The neighboring scan area in the "Area 1 → Area 2 → Area 3 → Area 4" order can create scan paths that have new arrangement storing ashes. As can be seen in Fig. 7, the scan path created using this approach reduced the jump section remarkably. The generation of the scan path can be decided simply on the basis of the number of scanning lines that are straight.

Fig. 8 shows the scan path generation algorithm based on the area division. First, the number of marks from most boundary blocks on one side to those on the other side in a straight line of scan rays is determined, and creates the area. The scan ray by neighbor order in the created area is rearranged and stored in a changing order, and all the other jumps are erased. Also, the minimum area of the region is limited to prevent it from dividing into small areas.

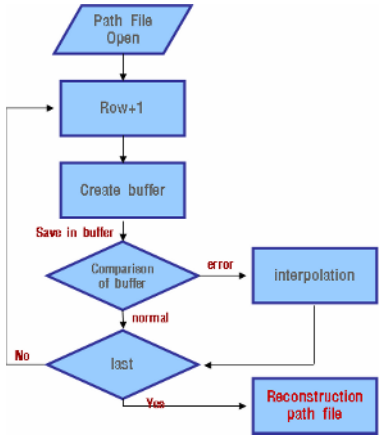

Fig. 9. Verification of the flow chart.

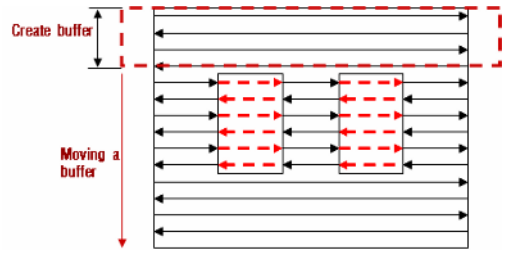

Fig. 10. Verification of the scan path algorithm.

3.3 Debugging algorithm of the simple-zigzag scan path

In the generation algorithm of the area division scan path, the exact number of marks in a straight line should be determined so that the correct area division would be attained. As such, a neutral file is created to verify the existing path file and to eliminate the error in the scan path file as regards the division of the exact number of marks. The scan path generation algorithm based on area division is applied through the verified neutral file.

In the scan path verification method, such as that shown in Fig. 9 and Fig. 10, the first buffer generates more than the minimum value, stores data, compares each line, and checks the regularity and errors. If a singularity of error and regularity are discovered here, the scanning line where an error occurred should be modified, and the verified neutral file is generated through addition, deletion, and rearrangement, according to each occasion. The scan path verification can create a confident scan path when the algorithm is applied for detailed scan path control and for the area division debugging of the basic scan path.

3.4 The area division scan path that considers the scan time algorithm

Since the laser scans while the powder is being sintered, the temperature of the sintered area is much higher than that of its surroundings. As such, the sintered part emits heat in all directions until the surrounding temperature reaches equilibrium. Eq. (5) shows energy q, which is radiated by the surroundings, where h_c is the heat transfer coefficient for convection, h_r is the heat transfer coefficient from radiation transmission, and Ts and T_a depict the chamber temperature and the temperature of the sintered bed, respectively [12]. The heating radiation continues until the chamber temperature and the temperature of the sintered part become the same.

$$q = A_s(h_c + h_r)(T_s - T_a) \tag{5}$$

Since the thermal radiant energies in Eq. (5) are emitted to the neighborhood until the temperature of the chamber and the temperature of the sintered part become the same, the heat that is emitted affects the sintering rate of the part that has not been scanned by the laser. When the energy is given and if the time is extended, the sintering rate by time in Eq. (6) increases [12].

$$\ln\left[\frac{h}{h_0}\left(\frac{h_0 - h_\infty}{h - h_\infty}\right)\right] = k't \tag{6}$$

When the scan time of an area divided through the simple scan path generation method is prolonged, the area interval composite plane becomes weak or can be distorted by the distribution of heat.

In a simple scan path, such as that shown in Fig. 11, when the scan path is scanned from area 2 to area 3, distortion occurs in the composite plane between area 1 and area 3, owing to the increase of the sintering rate due to thermal radiation as the scan time of area 2 is prolonged. This can decrease the composite plane's strength and accuracy. Thus, when the fixed scan time in Fig. 12 is exceeded, the creation of scan path generation that considers scan time moving to the following scan preserve is necessary.

The area division method that considers the scan time limits the absolute maximum scan time of the area when such area is divided into more than two parts, as shown in Fig. 12. However, the jump time increases if the area is divided into small parts. The method that limits the scan time of the area prolongs the total scan time compared to the algorithm of the area division, but it can confirm the strength and accuracy of the composite plane between areas. That is, the correlation between strength and accuracy elevation on one hand, and scan time on the other, which can be shown by using the suggested method, will

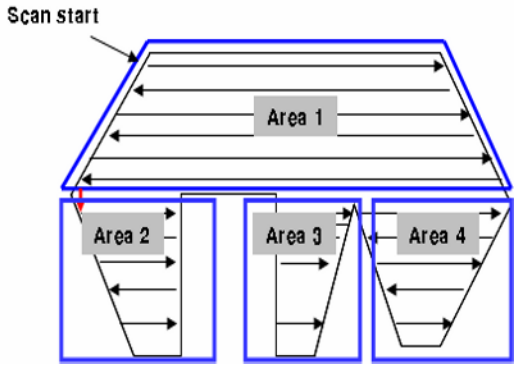

Fig. 11. Reconstructed scan path.

Table 1. Specification of polyamide powders.

	Particle size average(㎛)	Melting point(℃)
PA-12 powder	40-50	184

Table 2. Sintering condition of samples.

	PA-12
Temp(℃)	178
Scan speed(m/s)	6
Scan space(mm)	0.3
Laser power(W)	18
Layer thickness(mm)	100

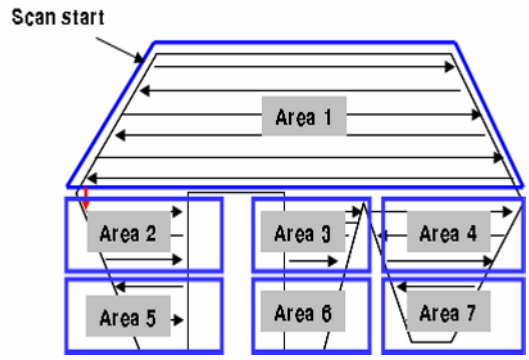

Fig. 12. Scan path algorithm for use in area division that considers the scan time.

necessitate much discussion and empirical analysis through an experiment that can consider the variables of Eq. (5) and Eq. (6).

3.5 Process condition of the powder

The PA-12 powder was used for the process. Table 1 shows the powder specifications and sintering condition that were used in the experiment [13]. This experiment found the sintering condition of powder by changing experimental conditions such as powder surface preheat temperature, laser power, and layer thickness. The powder surface preheat temperature decided a sintering point of 5~8℃ lower temperature than the powder melting point. Laser power and layer thickness were evaluated according to correlation of the sintering rate and preheat temperature of powder

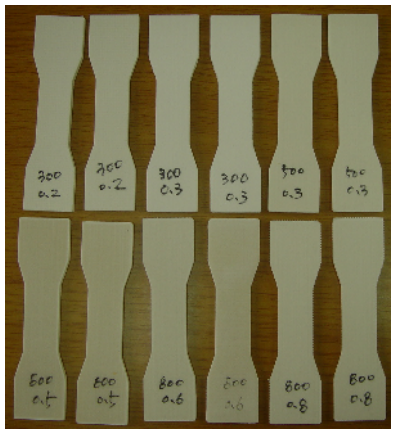

Fig. 13. Fabricate specimens.

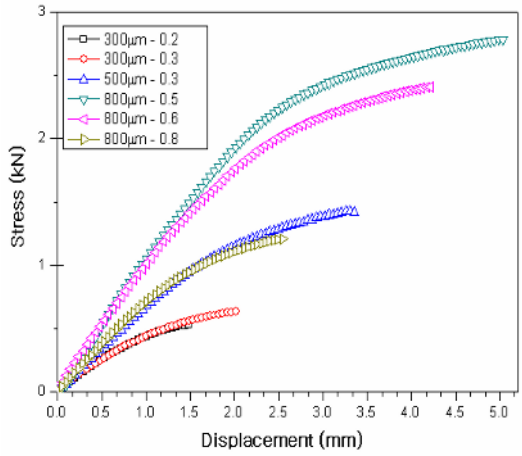

Fig. 14. Tensile test.

surface each. Table 2 shows the process condition determined through the experiment.

To verify the process condition shown in Table 2, the optimal process was determined through tensile test of specimens. These optimal processes lead to heat equilibrium between areas, the reduction of process time and improvement accuracy and process efficiency.

Fig. 13 displays specimens manufactured for applying process variables. This experiment obtains optimal spot size, spacing and scan speed through tensile test of specimen. The tensile test was performed by INSTRON 5583 Universal Testing Machines. The measured result is shown in Fig. 14, and Table 3 shows the experimental condition. Experimental results were obtained higher than the necessary minimum tensile 0.5kN of the prototype. Scan spacing can

Table 3. Experimental conditions.

Scan speed(m/s)	Layer thickness (μm)	Laser power(W)	Scan space(mm)
7	100	18	0.2
			0.3
5			0.3
2			0.5
			0.6
			0.8

be determined as more than 300 ㎛. Also, optimal spacing can be obtained to get each spot size, scan speed and laser power.

4. Comparison simulation and experiment on scan time

4.1 Scan control program and simulation on scan time

To compare the scan time with the simple scan path, or the area divided by the scan path and the area divided by the scan path that considers the scan time, the calculation algorithm of the scan time in the scan control program was embedded in and compared with the scan time. Fig. 15 shows the developed scan control program. The time efficiency of each algorithm was confirmed through the time simulation as a scan model 90×90×100-mm polygon model.

Fig. 16 compares the time of the jump section of the total layer with the result of the simulation. As shown in Fig. 16, the time of the model was shortened by about 307 seconds, such as when the existing scan path was changed to the area division scan path. Also, it is evident that the time was shortened by about 238 seconds when the algorithm that considers the scan time was used. It was confirmed that much scan time was saved, although the amount of time that was saved differed depending on the jump area and the laminating layer of the model.

4.2 The manufactured model

Fig. 17 shows the models that were fabricated according to the simulation model by using SFFS. The picture displays the fabricated parts that were produced by different scan path algorithms, such as (from the left) the simple scan path, the area division

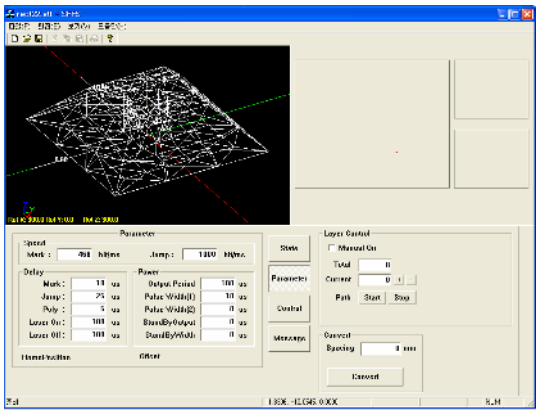

Fig. 15. Scan control program.

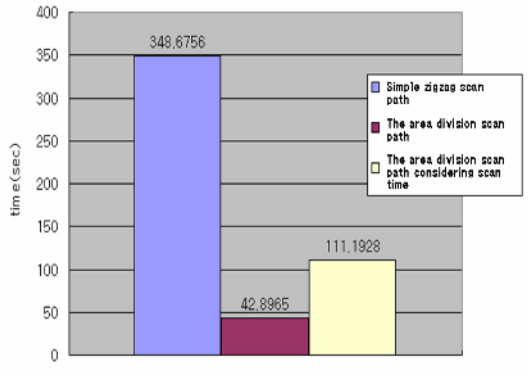

Fig. 16. Total jump time.

scan path, and the area division scan path that considers the scan time.

In an actual experiment where three algorithms were used, the differences among them were not clearly shown when observed with the naked eye. This is because the scan time between areas was short. In the sintering-rate-change experiment by time, the change in the sintering rate by time was considerable when about two minutes passed [8]. However, the suggested scan path algorithm that considers the scan time will most probably be used in actual manufacturing because much time will be consumed when the models used are bigger and have more complex shapes than the models used in the experiment conducted here in.

Fig. 18 shows the model that was used to observe the composite plane and the boundary through a microscope capable of 50 magnifications, which was manufactured by using the area division scan path algorithm. It was observed that distortion occurs when the composite plane of the area is more sintered. Fig.

Fig. 17. The manufactured model on which SFFS was used.

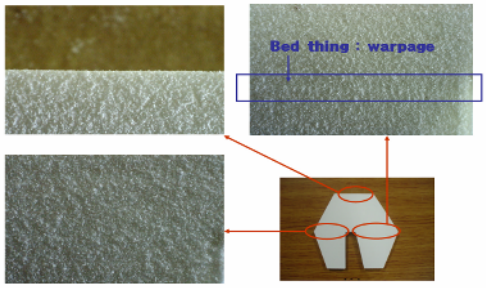

Fig. 18. The manufactured model that used the area division scan path (50-magnification microphotograph).

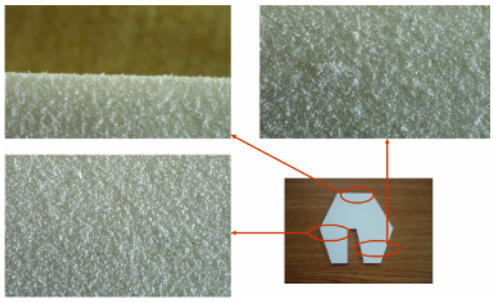

Fig. 19. The manufactured model that used the area division scan path that considers the scan time (50-magnification microphotograph).

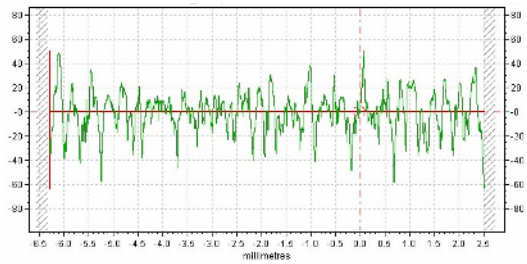

Fig. 20. Surface roughness measurement.

19 also shows the model that was manufactured by using the scan path algorithm that considers the scan time. When the same joint was observed under a microscope, no singularity was found. Fig. 20 shows the surface roughness measurement of interfacing area the model area division scan path that considers the scan time used the better surface roughness than the model area division scan path algorithm.

This can be attributed to the fact that the distortion decreased, thereby reducing the sintering-rate increase according to the time of the joint. Moreover, the area division scan path that considers the scan time limits the width of the area by limiting the absolute maximum scan time of the area. This may become a big advantage of the digital mirror system when applied to SFFS, as it can propose an optimized scan speed for the system, as well as scan spacing, which can limit the width of the areas to be sintered.

5. Conclusion

A method that creates scan paths by employing area division and that considers the scan time from a simple-zigzag scan path was developed to improve the laser scan efficiency in SFFS. The suggested method was evaluated by verifying the simple-zigzag scan path. Since the simple-zigzag scan path contains an unnecessary jump section, the mark number of the area was distinguished, and each area in the polygon was reconstructed to minimize the jump sections. Furthermore, models were manufactured that improved the scan efficiency when the scan path that considers the scan time was used. This method significantly decreases the distortion of the composite plane between n the areas as well as the strength of the sintered parts, which can occur as scan path generation problems of the area division scan path algorithm. Finally, it was applied to SFFS, and the fabricated models were observed and compared. It was confirmed from the experiment that was conducted in this study that the sintering-rate increase according to time affects the product.

Further studies must be conducted where the interrelationship of the scan time with the distortion and the strength of the area's composite plane could be further investigated with the use of models manufactured using the method proposed in this study. Further empirical analysis should be conducted in many more experiments by using the method proposed in this study, particularly about the effects of the use of the

method on the accuracy of the manufactured article.

Acknowledgment

This work was supported by the Korea Foundation for International Cooperation of Science & Technology(KICOS) through a grant provided by the Korean Ministry of Education Science & Technology (MOST) in 2009 (No. M60602000002-06E0200-00210).

References

[1] C. K. Chua, K. F. Leong and C. S. *Lim, Rapid Prototyping: Principles and Applications*, 2nd Ed. World Scientific Publishing, (2003).

[2] S. M. Hur, Generation of CAD Data for Rapid Product Development in Reverse Engineering. *Ph.D. dissertation, Pusan National University Graduate School*, (2002).

[3] H. C. Kim, Internet-based Intelligent CAD/CAM System for Rapid Product Development. *Ph.D. dissertation, Pusan National University Graduate School*, (2003).

[4] K. Chen, Intelligent scanning in selective laser sintering, *The University of Texas at Austin, Ph. D. Thesis*, (1998).

[5] S. M. Park, Advanced Data Exchange for Solid Freeform Fabrication, *The University of Texas at Austin, Ph. D. Thesis*, (2000).

[6] J. Yang, M. Bin, X. Zhang and Z. Liu, Fractal scanning path generation and control system for selective laser sintering(SLS), *International Journal of Machine Tools & Manufacture*, 34 (2003) 293-300.

[7] Y. H. Yang, T. J. Loh, H. Fuh and Y. G. Wang, Equidistant path generation for improving scanning efficiency in layered manufacturing, *Rapid Prototyping Journal*, 8 (1) (2002) 30-37.

[8] J. W. Choi, K. H. Choi, Y. H. Doh, D. S. Kim and Y. J. Ahn, A Study on the Generation of Laser Scanning Paths and Scanning Control. *Proceedings of the KSMPE Spring 2005 Conference*, Masan, Korea, 277-281, (2005).

[9] K. H. Choi, J. W. Choi, Y. H. Doh, S. J. Cho, S. H. Lee, Y. J. Ahn and D. S. Kim, Generation of Dual-Laser Scan Paths for the Enhancement of Mechanical Strength. *Proceedings of the KSME Fall 2005 Annual Meeting*, Gumi, Korea, 1074-1079, (2005).

[10] J. W. Choi, K. H. Choi, D. S. Kim, Y. H. Doh and S. H. Lee, Fabrication of Parts and Its Evaluation Using the Dual-Laser Solid Freeform Fabrication System. *Trans. of the KSME(A) paper*, 30 (3) (2006) 334-341.

[11] K. H. Kim, J. W. Choi, Y. H. Doh, S. H. Lee and D. S. Kim, Generation of Scan Paths for the Enhancement of Fabrication Efficiency in SFFS. *Proceedings of the KSME 2006 Spring Annual Meeting*, Jeju, Korea, 623-627, (2006).

[12] J. C. Nelson, Selective Laser Sintering: A Definition of the Process and an Empirical Sintering Model. *UMI*, (1994).

[13] Y. G. Bang, K. S. Choi, C. H. Park, H. I. Kim, B. S. Lim and D. S. Kim, Development of New Polymer Powders for the Industrial SFF system by using SLS Process *Proceedings of the KSME 2007 Spring Annual Meeting*, 1973-1978, (2007).

Kyung-Hyun Choi received his B.S. and M.S. degrees in Mechanical Engineering from Pusan National University, Korea, in 1983 and 1990, . He then received his M.S. and Ph.D. degrees from University of Ottawa in 1995. Dr. Choi is currently a professor at the School of Mechanical Engineering at Cheju National University, Korea. His research interests include micro-machining, printed Electronics.

Yang-Hoi Doh received his B.S. and M.S. degrees in Electronics Engineering from KyungBuk National University, Korea, in 1982 and 1984, respectively. He then received his Ph.D. degree from University of Kyung Buk National University, Korea, in 1988. Dr. Doh is currently a Professor at the School of Electronics Engineering at Cheju National University, Korea. His research interests include micro-machining, Digital signal processing.

Hyung-Chan Kim received his B. S. and M. S. degrees in Electronics Engineering from Cheju National University, Korea, in 2006 and 2008, respectively. Mr. Kim is currently a Ph.D. candidate at the School of Electronics Engineering at Cheju National University, Korea. His research interests include RP System, micro-machining, printed Electronics.

Dong-Soo Kim received his M.S. and Ph.D. degrees in Mechanical Engineering from Yung Nam University, Korea, in 1991 and 2001, respectively. Dr. Kim is currently the general manager at Nano Mechanical System Research Division at Korea Institute of Machinery & Materials. His research interests include printed Electronics, R2R printing, RP system.